



ELSEVIER

Journal of Alloys and Compounds 300–301 (2000) 11–17

Journal of
ALLOYS
AND COMPOUNDS

www.elsevier.com/locate/jallcom

Coherent light sources with powder: stimulated amplification versus super-radiance

François Auzel*, Philippe Goldner

Groupe Optique des Terres-Rares, CNRS, UPR 211, 1 place A. Briand, 92190 Meudon, France

Abstract

Though the common laser sources usually make use of optically non-scattering materials, the basic processes involved in the generation of coherent light by either ASE (amplification of spontaneous emission by stimulated one) or by synchronised spontaneous emission, namely super-radiance and superfluorescence, do not require transparent materials. In this paper, results from the literature and from our own work on ASE and on superfluorescence processes obtained on rare-earth-doped powdered materials are presented with emphasis on our recent new results on super-radiance in powder samples. A critical discussion of these results is presented with reference to existing theories of gain in diffusing media. It is shown that when stimulated amplification is taking place, several grains with centimeter long path are involved, whereas when super-radiance is observed only one grain is sufficient for the process, provided that conditions on T_2 are respected. © 2000 Elsevier Science S.A. All rights reserved.

Keywords: Phosphors powders; Optical properties; Laser; Super-radiance; Coherent elastic light scattering

1. Introduction

Ideas about laser effects in scattering media are already old, since they can be traced back to the theoretical paper in 1966 by Letokhov [1] and to a first experiment in 1971 by Varsanyi [2] on a single grain of PrCl_3 , a fully concentrated material. However, real powder systems have been considered in a more systematic way only recently [3–7]. In parallel with this field, recent results obtained for laser action in dye solutions with passive scattering powder [8] have pushed forward new theoretical investigations on gain in scattering medium in connection with photon localisation [9] by the disordered medium and on coherent back scattering (CB) of light from amplifying medium [10].

In the following, we shall first review amplification by stimulated emission (ASE) and laser effects with active powders as observed under high peak power at low (77 K) [3,4] and room temperature [6,7]. Such types of results needs rather high concentrations of $\sim 10^{21}$ – 10^{22} cm^{-3} of active ions in order to obtain thresholds in the range of 2×10^5 – 10^9 W/cm^2 .

We shall then discuss the superfluorescence effect, in the Bonifacio sense, that we have obtained on powder [11]. This effect is in marked contrast with ASE, since here low

concentrations, $< 10^{20}$ cm^{-3} , are required providing, under continuous excitation (CW), very low density thresholds of about 10^3 W/cm^2 from 10 to 60 K [12]. Finally we shall present here our latest results for the super-radiance of Er^{3+} , observed on a single layer of powder with grain diameter of 30 μm .

2. Amplification by stimulated emission (ASE) and lasers with powders

2.1. Laser effect in powders of stoichiometric and Nd-doped laser materials

The first experiments of laser on powders have been obtained on so-called stoichiometric laser materials of $\text{Na}_5\text{Nd}(\text{MoO}_4)_4$, $\text{LiNd}(\text{PO}_3)_3$, $\text{NdP}_5\text{O}_{14}$ [3,4]. Such a family of materials, with the active rare earth ion as a constituent of the host, were well known in the late 1970s as laser materials with tens of microns size active length [13]. Such an effect was then extended by the Russian group to a wider range of Nd-doped materials such as La_2O_3 , $\text{La}_2\text{O}_2\text{S}_5$, La_3NbO_7 and SrLa_2WO_7 [5].

All these results have been obtained at 77 K, with threshold from about 2×10^5 to 3×10^6 W/cm^2 for grain diameters ranging from 250 μm to 10 μm and Nd^{3+}

*Corresponding author.

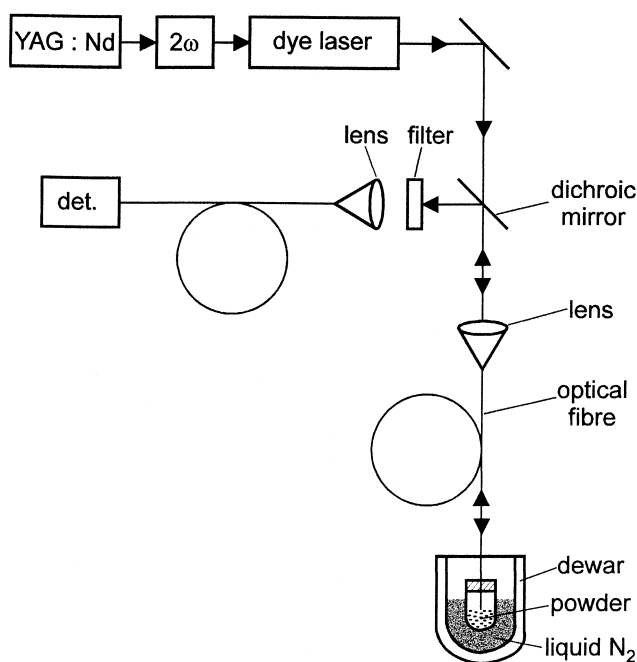


Fig. 1. Typical experimental set-up for a powder laser at liquid nitrogen temperature, from Ref. [3].

concentrations between 10^{21} and 4×10^{21} cm^{-3} . Fig. 1 shows the typical experimental set-up.

More recently, room temperature laser effect have been obtained under pulse excitation for Nd again in highly doped or stoichiometric powder materials with concentration above 10^{21} cm^{-3} in $\text{La}_{1-x}\text{P}_5\text{O}_{14}\text{-Nd}_x$, $\text{NdCl}_3 \cdot 6\text{H}_2\text{O}$ with threshold of 10^9 W/cm^2 and in $\text{NdAl}_3(\text{BO}_3)_4$, $\text{NdSc}_3(\text{BO}_3)_4$, $\text{Sr}_5(\text{PO}_4)_3\text{F-Nd}$, with threshold above $1.7 \cdot 10^7$ W/cm^2 [7]. An example of the pulsed behaviour of the emission below and above laser threshold for $\text{NdCl}_3 \cdot 6\text{H}_2\text{O}$ is given in Fig. 2.

For all these results the laser criterion is that above a pump threshold, a strong line narrowing is observed together with a pulsed time decay with time constants

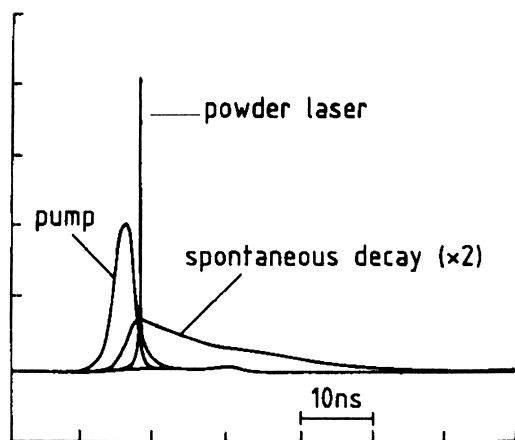


Fig. 2. Pulsed emission from $\text{NdCl}_3 \cdot 6\text{H}_2\text{O}$ powder at room temperature below and above laser threshold, from Ref. [28].

shorter than the spontaneous emission life-time. The integrated output signal is linear with pumping above the threshold.

2.2. ASE in materials with coherent backscattering

Besides gain in powder medium, the so-called coherent backscattering effect (CB) on passive scattering powder has been discovered and investigated [14–16] at first independently of active powders and now in conjunction with active powders [10].

The CB or case of photon ‘weak localisation’ can be understood by recognising the fact that any random path of light inside a scattering medium, coming back to its impinging point can be ‘time reversed’ that is can be followed the other way round. Those two waves on coming back interfere constructively whatever the randomness of the path.

All other paths, not respecting the k -vector conservation law

$$-k_m = k_0$$

vanish by destructive interference according to the phase mismatch caused by angle θ between k_m and k_0 , where k_0 is the incident wave k -vector and k_m is the k -vector after the m th scattering event. The error on the phase mismatch is given by the average distance between the first and last scatterer that is also the mean free path between two successive scattering events, l . The corresponding dephasing is given by

$$\Delta\Phi = 2\pi \frac{\lambda}{l} \theta \quad (1)$$

where θ is the scattering angle with respect to the normal incidence, see Fig. 3.

Then it can be shown that the coherently enhanced backscattered ‘cone’ which is a Gaussian function shall have an angular width at half intensity given by [14]

$$2\theta_{1/2} = \frac{3}{4} \pi \frac{\lambda}{l} \quad (2)$$

where λ is the light wavelength.

It has been experimentally shown that when the medium between the scattering objects is absorbing, for instance rhodamine 6G solution with scattering polystyrene spheres, the CB cone flattens [17]. In fact, because the cone maximum corresponds to the longest paths, they are just the ones which are the most reduced by absorption, though the scattering mean free path keeps the same.

It is not a surprise that the opposite behaviour is obtained when gain is provided inside the scattering composite medium. Both theory [18] and experiments [10] have recently shown that the CB cone is narrowed by gain together with a rising of the background for larger angles as shown in Fig. 4. This last experiment has been obtained in a pump-probe configuration in order to measure the CB

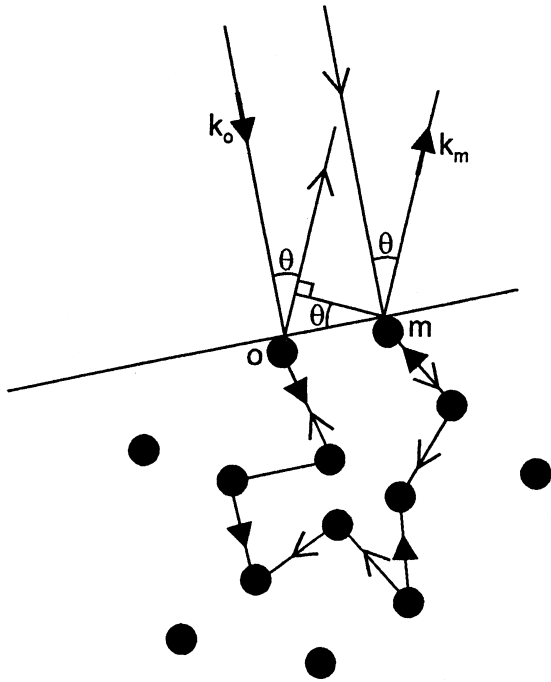


Fig. 3. Dephasing of scattered vector k_m in coherent backscattering for an angle θ from incident beam with vector k_0 .

cone at the probe wavelength with or without pumping of the scattering powder made of 0.15 wt% Ti_2O_3 in Al_2O_3 (titanium sapphire powder) either dry or in a water suspension. The ASE gain and CB cone are measured using a common frequency doubled Nd–YAG laser pumping both a regular Ti–sapphire laser providing the probe signal, and the amplifying active scattering powder itself.

This first experiment of controlled ASE amplification in a scattering powder does not present of course the threshold of a laser effect. Shortly afterwards, this experiment has been extended by the same group to a systematic study of the gain in Ti–sapphire powder and of other random media such as ruby powder in air or in glycerol [19].

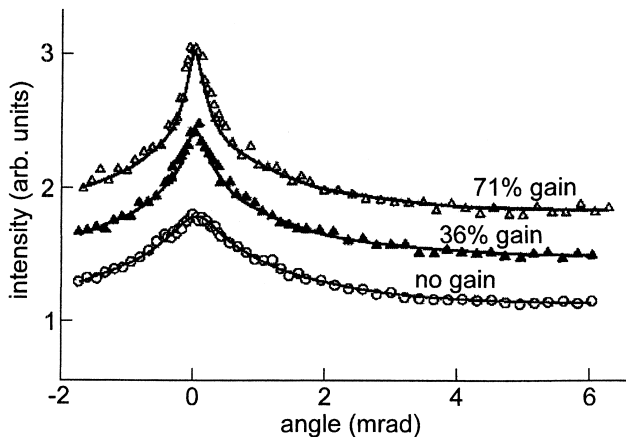


Fig. 4. Coherent backscattering in Al_2O_3 –Ti active powder, from Ref. [10].

3. Superfluorescence and super-radiance in powders

3.1. Observation on bulk and large grain powders [11]

A somewhat analogous behaviour to ASE has been obtained, for emission at $2.7 \mu\text{m}$ (${}^4\text{I}_{11/2} \rightarrow {}^4\text{I}_{13/2}$ transition), on powder of LiYF_4 –Er with large grain ($> 100 \mu\text{m}$) [11] and now extended down to $30 \mu\text{m}$ as presented here.

However, the experimental conditions which prevail for the effect we are going now to describe are rather different from the one which were necessary for ASE in scattering media as just seen. The experimental set-up is just the one usually used for recording a luminescence spectrum.

The super-fluorescence effect can be viewed as the radiative coupling during T_2 of one ion, S_i , with another one nearby as depicted in Fig. 5 by their Bloch sphere. When all ions in the samples are in phase, they emit coherently as a single ‘macro-dipole’, the size of which is proportional to the number of coherently coupled ions. This provides an intensity proportional to the square of a dipole that is now proportional to the square of the number of excited ions in phase.

Here, contrary to ASE, concentration of active ions have to be kept low ($< 10^{20} \text{ cm}^{-3}$) in order to maintain T_2 as large as possible; the observed threshold for line narrowing and spiking behaviour for the output signal is very low ($< 10^3 \text{ W/cm}^2$) and can be obtained by CW krypton laser excitation; temperature cannot exceed about 60 K and the thermal behaviour for threshold is linked with a phonon direct process reducing the T_2 of the emitting lowest Stark level (see Fig. 6) [12]; integrated output signal is quadratic with pumping above threshold.

All these facts point to a superfluorescence or super-radiance effect in the Dicke–Bonifacio sense [20], that is to a collective effect of excited states for which the principal condition is the existence of a T_2 , the dephasing time, larger than the superfluorescence lifetime.

On the contrary, conditions on T_2 are not a prerequisite for ASE. On the other hand, one knows that large T_2 are linked with low temperature and weak concentration. This is opposite to researching large gain in optical short paths as for ASE amplification.

3.2. Observation on powder with grain diameter of $30 \mu\text{m}$

By direct excitation into the ${}^4\text{I}_{11/2}$ of Er, with a Ti–sapphire CW laser, we have now obtained the super-fluorescence effect (super-radiance) down to grain diameter of $30 \mu\text{m}$ on a single layer of grains as reported here. Fig. 7 gives the emission spectrum below and above threshold, which for 9666 \AA excitation, is 827 W/cm^2 at $T = 11 \text{ K}$. The observed excitation spectrum of Fig. 8 reveals the six Stark levels of ${}^4\text{I}_{11/2}$ in the electric field of the local site of Er in LiYF_4 plus two replica at 9742 and 9755 \AA

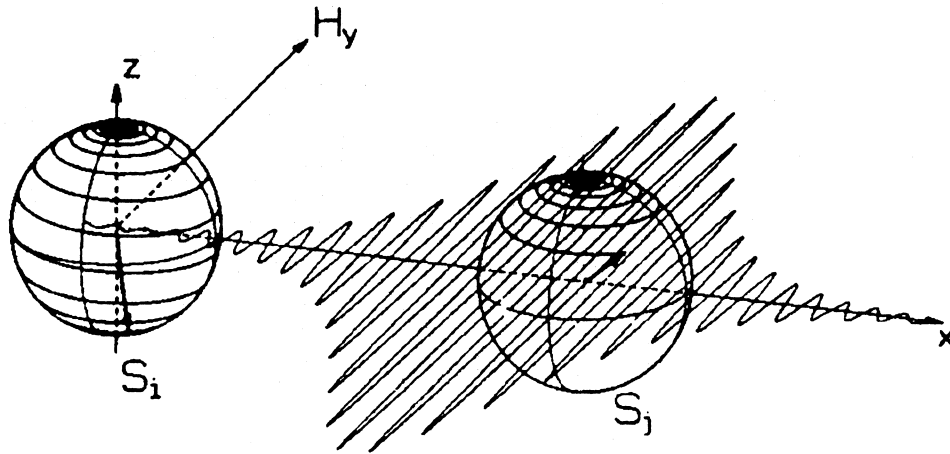


Fig. 5. Self-synchronization of nearby ions S_j by field coupling with S_i , represented by their Bloch sphere, in super-radiance emission; H_y is the common direction of Bloch vectors in both spheres; from Ref. [29].

corresponding to the ${}^4I_{15/2}$ first Stark level slightly populated at 11 K.

Chopping the pump beam with a long period of 80 ms, below and above threshold, allows the observation of the temporal behaviour of the super-radiant emission, see Fig. 9. Below threshold, only the usual spontaneous emission is observed; above threshold, a much shorter spike is observed the intensity of which shows a quadratic behaviour shown in Fig. 10.

Though the threshold power density is about the same

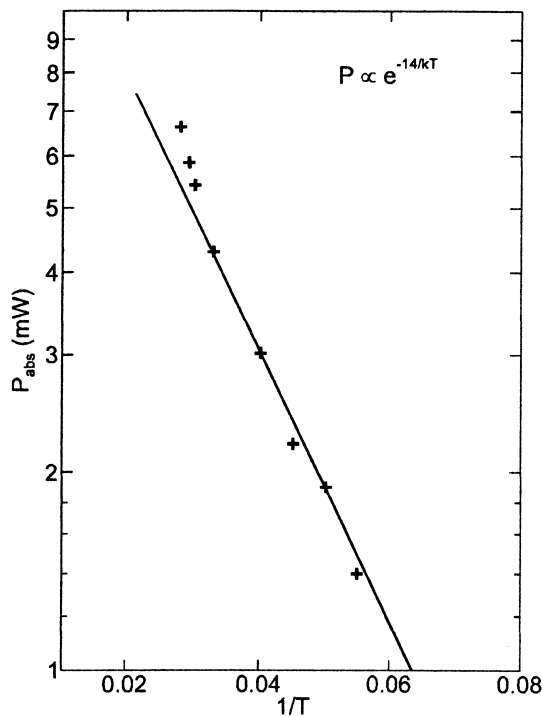


Fig. 6. Threshold temperature dependence for superfluorescence of $\text{LiYF}_4\text{-Er}$; activation energy corresponds to the first Stark splitting of ${}^4I_{15/2}$; after Ref. [12].

for the large grain and the small grain cases, the fact that now we observe super-radiance on the powder with a smaller diameter grain than before, is attributed to the fact that the pumping photons are now directly used to create the excited state density. With the Argon laser excitation of Ref. [11], the ${}^4F_{9/2}$ state was first excited at 5110 cm^{-1} above the useful excited state; this energy had to be dissipated as phonons so heating the sample. Also the self-phasing of the spontaneous emission had to start from itself (super-fluorescence) whereas now the phasing of excitation can be used to start the phasing of emission from the lowest emitting Stark level (super-radiance). All these explains the better efficiency of the Ti-sapphire excitation we observe now. In particular, the fact that at a concentration of $2.1 \times 10^{21}\text{ cm}^{-3}$, super-radiance cannot be observed either in powder or in bulk whereas this is the optimised concentration for cw laser [21], clearly demonstrates the difference between the two processes described above in Sections 2 and 3.

4. Discussion

4.1. The laser effect in powders and photon localisation

Following Ref. [5], we can estimate the average necessary gain path l_a to explain the line narrowing observed in laser effects in powder. It is given by

$$l_a \approx \frac{\log_n(2)}{\alpha_0 \delta\nu/\Delta\nu} \quad (3)$$

where α_0 is the maximum gain coefficient, the laser emission width, the line width below threshold. In Ref. [5], with $\delta\nu/\Delta\nu=0.18$, $\alpha_0=10\text{ cm}^{-1}$, the average gain path by (3) has to be at least 2.3 cm. In our own case of powder

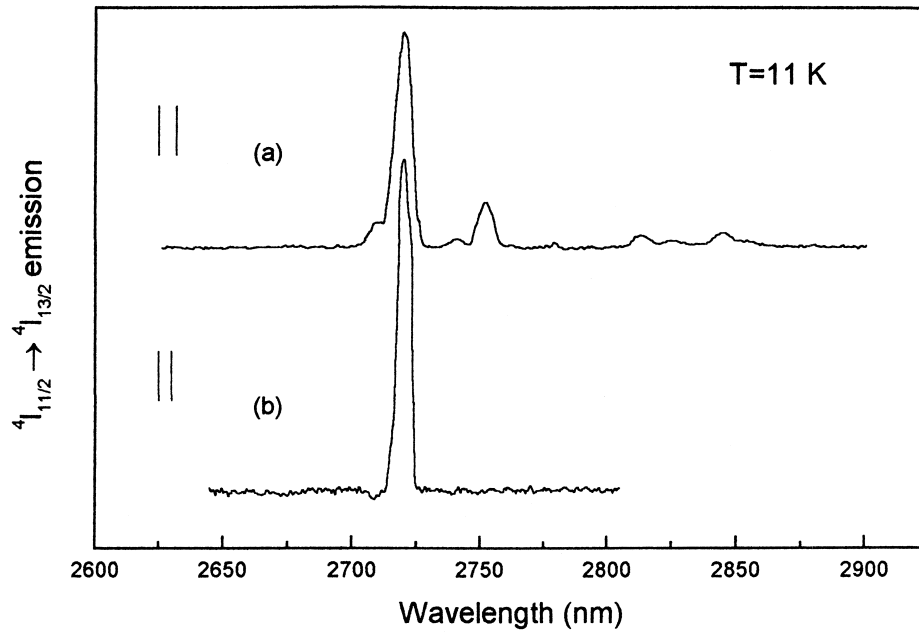


Fig. 7. Emission spectra below (a) and above threshold (b) of a single layer of LiYF₄-Er powder with grains diameter of about 30 μm.

laser [6] we had $\delta\nu/\Delta\nu = 5.3 \times 10^{-4}$, $\alpha_0 = 800 \text{ cm}^{-1}$ giving $l_a = 1.63 \text{ cm}$ above threshold. In both cases, one finds the same order of magnitude for the necessary path length. In Ref. [5] it was concluded that the laser effect was taking place with several grains along a close ring path each grain keeping the photons for a few total reflection paths within the microcavity constituted by the grain.

Such close rings of centimeter size are clearly not compatible with the close rings advocated in strong

localisation of light [22], because in the recent first demonstration of strong localisation [23], the requested scattering mean free path, l , is such that:

$$l \leq \frac{1.5\lambda}{2\pi\sqrt{n}} \quad (4)$$

where \sqrt{n} is the average index of refraction of the composite material made of air and particles of index n . For rare earth doped materials this comes to $l < 0.19 \mu\text{m}$

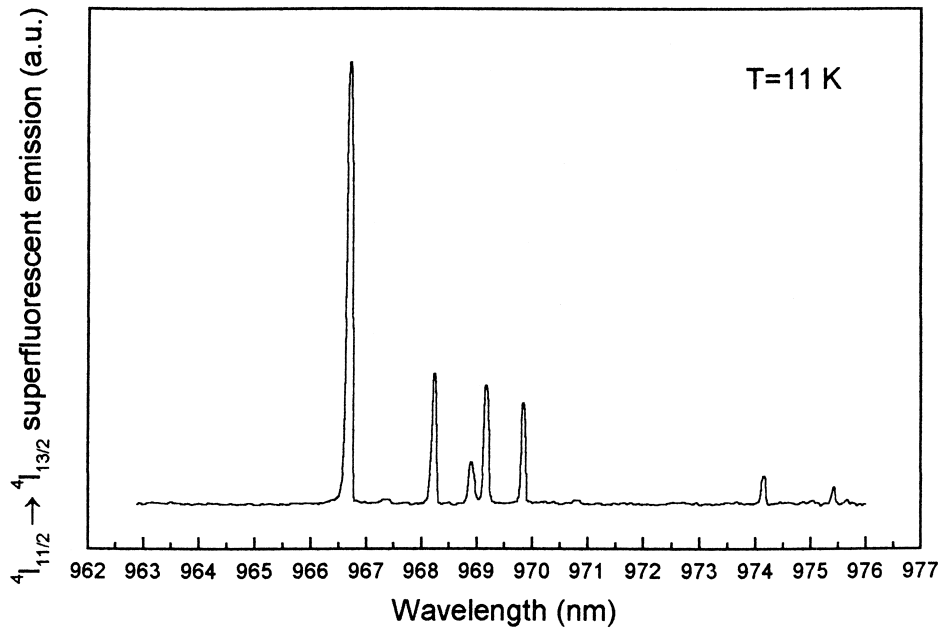


Fig. 8. A 2.7-μm superfluorescence excitation spectrum for the LiYF₄-Er powder.

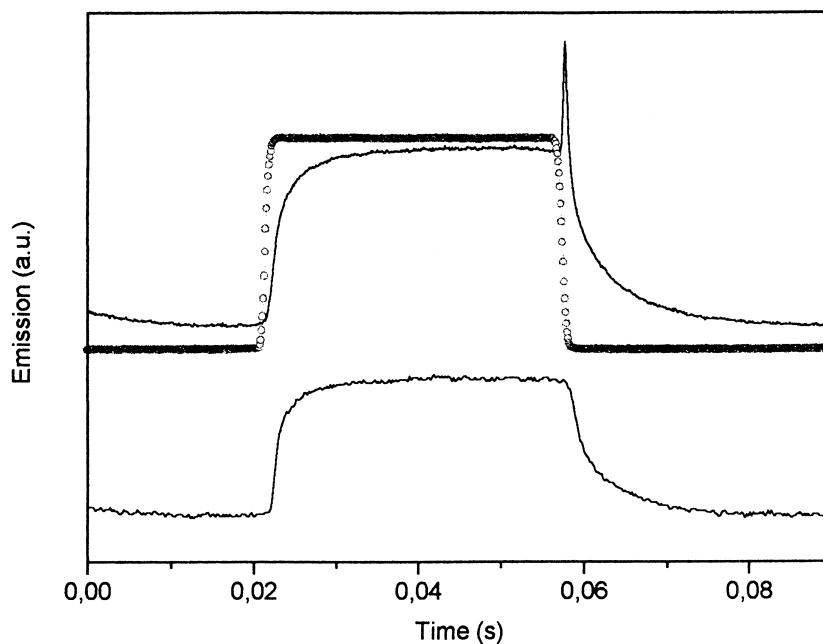


Fig. 9. Dynamical behaviour of ${}^4I_{11/2}$ emission below (lower trace) and above threshold (upper trace). The trace with open dots is the pump intensity. Note the superfluorescence spike.

which is much less than expected for grain diameters between 5 and 50 μm at close contact.

In our view a more realistic way to see the laser effect in powder is to consider the ‘time reverse’ paths considered in CB as the effective closed rings necessary to explain the observed spectral narrowing. By analogy with the theory for a scattering medium with absorption [17], we consider the scattering angle θ_a corresponding to a given gain length, l_a , for a weak localisation loop without dephasing

$$\theta_a = \left(\frac{3\lambda^2}{4\pi^2 l_a} \right)^{1/2} \quad (5)$$

For small angles such loops may be very long. For example, taking a scattering length $l = 10 \mu\text{m}$, $\lambda = 1.06 \mu\text{m}$, a single path gain of 1 cm is compatible with an angle θ_a of 0.92 mrd, typical value for CB experiments with gain (see Fig. 2).

On the other hand, all laser experiments scheme described to date on rare-earth doped powder laser [5,6], have in fact made use of a back-scattering detection scheme with an optical fibre. Then clearly θ_a is within the accepting angle of the detection path. For all these reasons we like to propose that powder lasers have to involve closed ring paths of the ‘time reverse’ type.

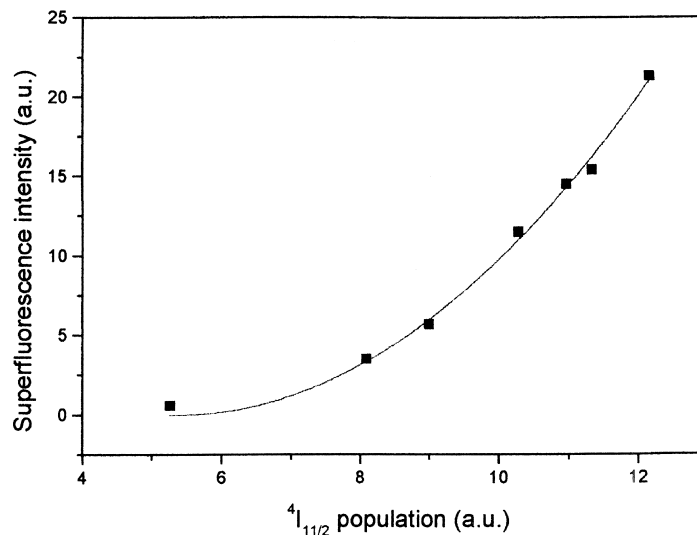


Fig. 10. Integrated intensity of the superfluorescence peak of Fig. 9 versus relative population density of emitting level ${}^4I_{11/2}$ as measured by the spontaneous emission intensity of Fig. 9. The continuous line is a quadratic fit.

4.2. Super-radiance in rare-earth doped powder materials

In order to discuss the super-radiance case, we have to first recall the dimensional conditions for super-radiance [11]. They are the following:

$$L_T \ll L \ll L_c \quad (6)$$

where L_T is a threshold critical length, L is the sample length, L_c is the Arecchi–Courtens cooperative length [24]. In case of pulsed pumping, $L < L_c$ insures that super-radiance emission gives a single pulse; when $L \cong L_c$, oscillatory behaviour is possible; in both cases output is proportional to ρ^2 (ρ is the excitation density) as observed in Fig. 7. For $L > L_c$, ASE would overcome super-radiance and output should be proportional to ρ . In Ref. [25], we had found, for the same material, a super-radiance decay time $\tau_R < 150$ ns. We can estimate $L_T = L\tau_R/T_2$ [26]. It means that the left hand side of (6) will be fulfilled for $\tau_R < T_2$, i.e. $T_2 > 150$ ns. This condition should be respected since T_2 values of about 300 ns to 2 μ s have been reported for same host with various rare-earth dopants [27]. The right hand part of (6) is always fulfilled in our case [11]. This discussion shows that, for our super-radiance experiment, individual grains of the powder are involved, and that scattering paths between different grains are not necessary. Not looking for gain paths, in turn explains the low acceptable concentration. Also large a T_2 necessitates a low concentration and the low temperature to avoid dephasing in the photon–ion interaction

5. Conclusion

We have clearly contrasted the behaviour of powder coherent sources involving ASE or super-radiance. In the former case, ‘time reverse’ paths have to be involved in order to insure the necessary long path in the scattering medium. Also large active ion concentration helps the process. In the second type of coherent sources, low concentration is necessitated and individual grains are involved.

There are a number of applications for these intrinsically low price powder coherent sources that have been proposed. For sources of the first type, highly stable frequency standard [1] had been first considered; also reduced coherence driver sources for fusion megajoule lasers, holography, transport of energy in fibres for medical applications [28,6]. As for super-radiance sources, because they are based on synchronisation of spontaneous emission

which constitutes the basic noise limitation in optical amplifiers, noise suppressed amplifiers have been considered [25] which could be extended to the powder case.

References

- [1] V.S. Letokhov, Soviet Phys. JETP 26 (1968) 835.
- [2] F. Varsanyi, Appl. Phys. Lett. 19 (1971) 169.
- [3] V.M. Markushev, V.F. Zolin, C.M. Briskina, Sov. J. Quantum Electron. 16 (1986) 281.
- [4] V.M. Markushev, N.E. Ter-Gabrielyan, C.M. Briskeva, V.R. Belan, V.F. Zolin, Sov. J. Quantum Electron. 20 (1990) 73.
- [5] N.E. Ter-gabrielyan, V.M. Markushev, V.R. Belan, C.M. Briskina, O.V. Dimitrova, V.F. Zolin, A.V. Lavrov, Sov. J. Quantum Electron. 21 (1991) 840.
- [6] C. Gouedard, D. Husson, C. Sauteret, F. Auzel, A. Migus, J. Opt. Soc. Am. B 10 (1993) 2358.
- [7] M.A. Noginov, N.E. Noginova, H.J. Caulfield, P. Venkateswarlu, T. Thompson, M. Mahdi, V. Osroumov, J. Opt. Soc. Am. B 13 (1996) 2024.
- [8] N.M. Lawandy, R.M. Balanchandran, A.S.L. Gomez, E. Sauvain, Nature 368 (1994) 436.
- [9] J. Sageev, P. Gendi, Phys. Rev. A 54 (1996) 3642.
- [10] D.S. Wiersma, M.P. Van Albada, A. Lagendijk, Phys. Rev. Lett. 75 (1995) 1739.
- [11] F. Auzel, S. Hubert, D. Meichenin, Europhys. Lett. 7 (1988) 459.
- [12] S. Hubert, D. Meichenin, F. Auzel, J. Lumin. 45 (1990) 434.
- [13] F. Auzel, Processes in heavily doped rare-earth materials and their applications to optoelectronic devices, in: M.A. Herman (Ed.), Semiconductor Optoelectronics, Wiley, New York, 1980.
- [14] M.P. Van Albada, A. Lagendijk, Phys. Rev. Lett. 55 (1985) 2692.
- [15] P.E. Wolf, G. Maret, Phys. Rev. Lett. 55 (1985) 2696.
- [16] Y. Kuga, A. Ishimaru, J. Opt. Soc. Am. A8 (1984) 831.
- [17] P.E. Wolf, G. Maret, E. Akkermans, R. Maynard, J. Phys. France 49 (1988) 63.
- [18] A.Y. Zyuzin, Europhys. Lett. 26 (1994) 517.
- [19] D.S. Wiersma, A. Lagendijk, Phys. Rev. E 54 (1996) 4256.
- [20] R. Bonifacio, L.A. Lugiato, Phys. Rev. A 11 (1975) 1507.
- [21] F. Auzel, S. Hubert, D. Meichenin, Appl. Phys. Lett. 54 (1989) 681.
- [22] P. Sheng, Scattering and Localization of Classical Waves in Random Media, World Scientific, Singapore, 1990.
- [23] D.S. Wiersma, P. Bartolini, A. Lagendijk, R. Righini, Nature 390 (1997) 671.
- [24] F.T. Arecchi, E. Courtens, Phys. Rev. A 2 (1970) 1730.
- [25] F. Auzel, Properties of highly populated excited states in solids: superfluorescence, hot luminescence, excited states absorption, in: B. DiBartolo (Ed.), Optical Properties of Excited States in Solids, Plenum Press, New York, 1992, p. 305.
- [26] H.M. Gibbs, Q.H.F. Vreken, H.M.J. Hiksloops, Phys. Rev. Lett. 39 (1977) 547.
- [27] G.K. Liu, M.F. Joubert, R.L. Cone, B. Jacquier, J. Lumin. 38 (1987) 34.
- [28] C. Gouedard, D. Husson, C. Sauteret, F. Auzel, A. Migus, in: IAEA Conf. On Drivers for Inertial Confinement Fusion, Osaka (Japan) April 15–19, 1991, paper E04.
- [29] L.O. Schwan, J. Lumin. 48/49 (1991) 289.